

Introduction

In this work, the optical properties of Au-Ag alloy nanoparticles (NPs) with an anthracene ligand grafted to their surfaces was examined. Structurally and chemically homogeneous Au-Ag NPs were synthesized by a seed-mediated method¹ with the Ag precursor reduced and grown onto the prepared Au seeds. The alloy NPs were formed after inter-diffusion of Au and Ag and protected using oleylamine. Functionalization of the metal NPs with the anthracene-incorporated ligands was conducted via a simple ligand exchange protocol². The morphological information and chemical composition of the resulting NPs were confirmed by transmission electron microscopy (TEM) and energy dispersive X-ray spectroscopy (EDS), respectively. The plasmonic effect of the metal NPs on the fluorescence was examined using Ultraviolet-visible (UV-vis) and fluorescence spectroscopy.

Synthesis of Au-Ag Alloy Nanoparticles

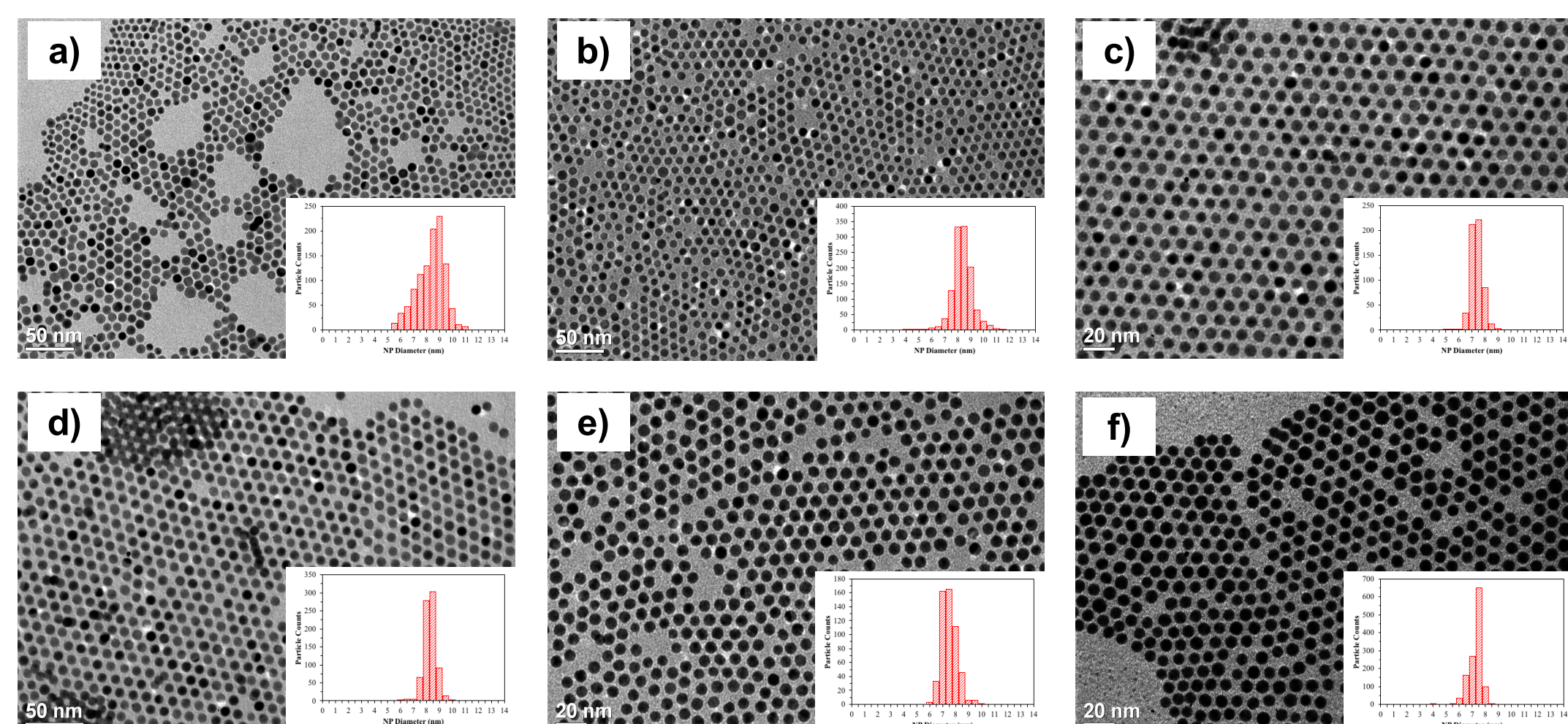


Figure 1. TEM images of $Au_xAg_{1-x}@Olam$ NPs (a) $AuAg_4$ (8.09 ± 1.06 nm), (b) Au_2Ag_3 (8.12 ± 0.78 nm), (c) Au_3Ag_2 (7.04 ± 0.43 nm), (d) Au_4Ag (8.04 ± 0.46 nm), (e) Au (7.00 ± 0.46 nm), (f) Ag (7.27 ± 0.58 nm).

A series of monodisperse $Au_xAg_{1-x}@Olam$ NPs ($0 \leq x \leq 1$) shown in **Figure 1** with six different compositions and nearly identical sizes were synthesized to probe how the plasmon resonance bands affect the absorption or emission bands of the anthracene. They are denoted as Ag, $AuAg_4$, Au_2Ag_3 , Au_3Ag_2 , Au_4Ag , and Au NPs based on the relative composition of each sample. The average diameter size of all the metal NPs is 7.5 nm (7.00 to 8.12 nm) and the size distribution ranges from 4 % to 13 %. The actual elemental ratio of the NPs was quantitatively determined using EDS (**Figure 2**) and is relatively close to the nominal composition. As the relative composition of Au increases, a redshift of the surface plasmon resonance band is observed in the UV-vis spectra (**Figure 3**).

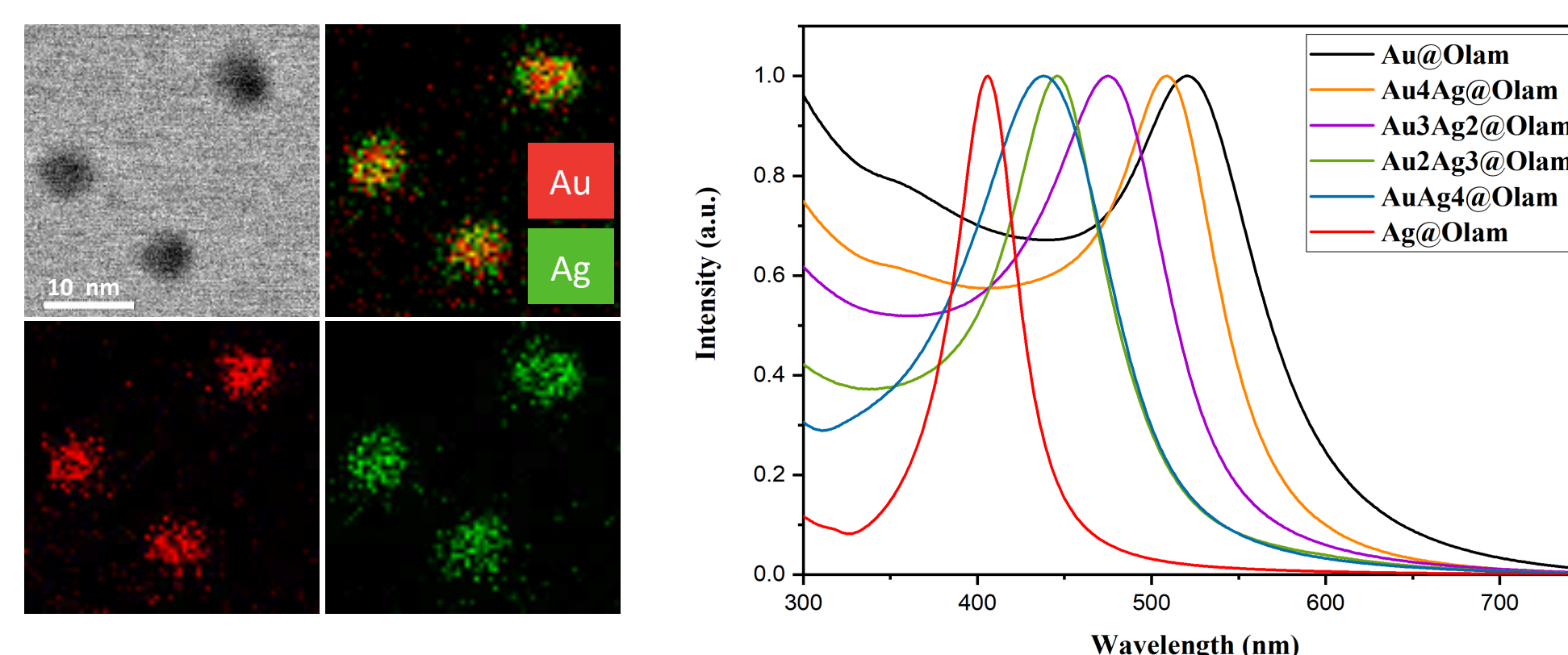


Figure 2. HRTEM image and **Figure 3.** UV-vis spectra of EDS elemental mapping of $Au_xAg_{1-x}@Olam$ NPs. $Au_2Ag_3@Olam$.

Functionalization of NPs with Anthracene Ligand

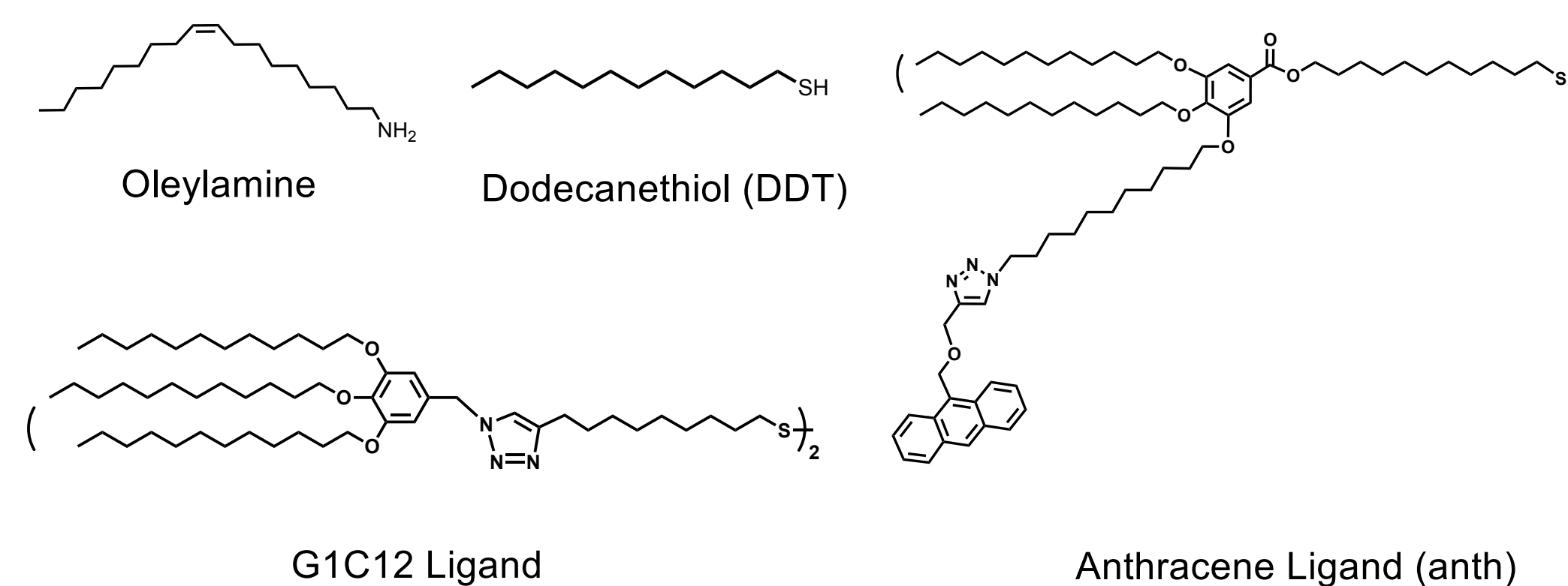


Figure 4. Molecular structure of ligands.

The ligands were grafted onto the NP surface via a ligand exchange procedure, in which the weakly coordinated oleylamine is replaced with thiolated ligands that have stronger bonding to the NPs. The completeness of the ligand exchange was determined using nuclear magnetic resonance spectra. The NPs after ligand exchange (~ 9 nm) generally exhibit improved colloidal stability compared with $Au_xAg_{1-x}@Olam$ NPs.

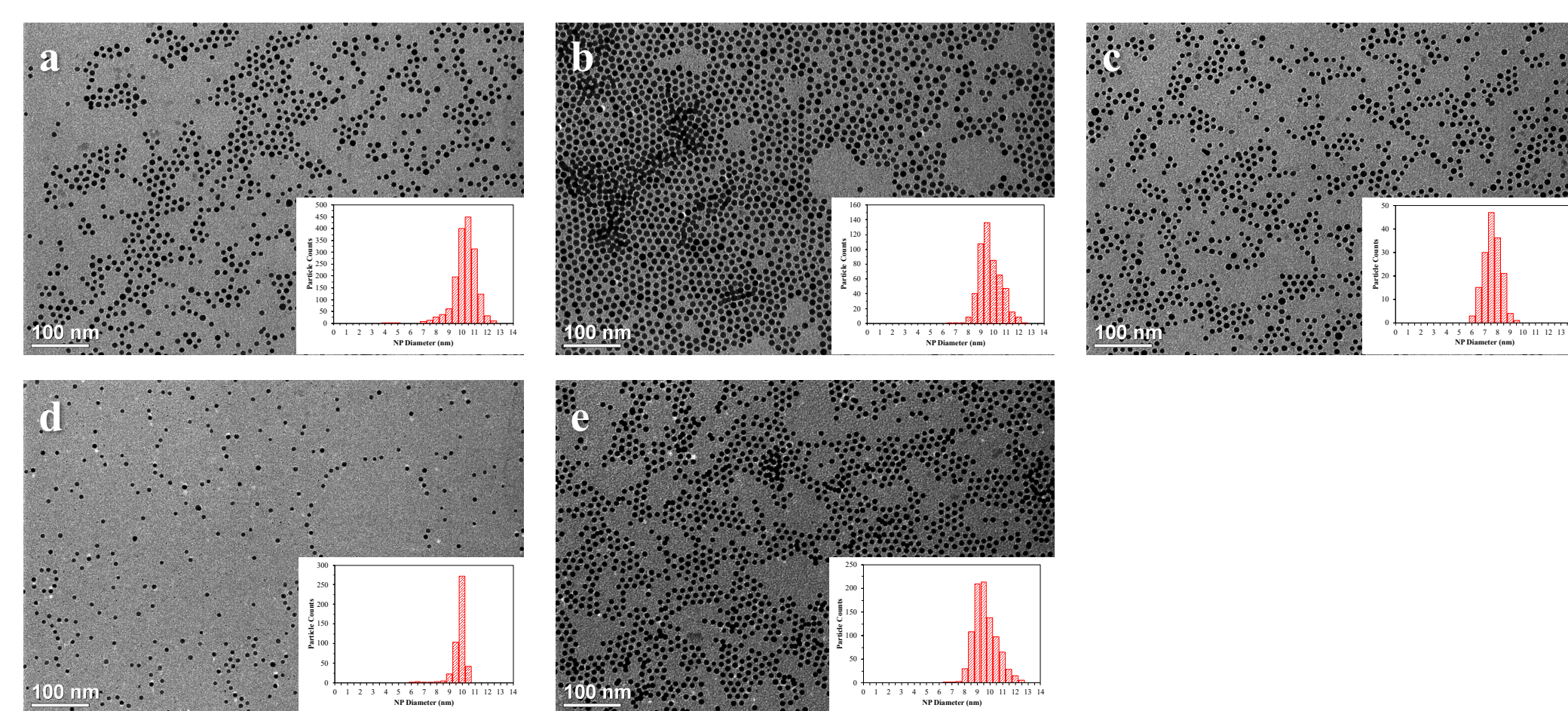


Figure 5. TEM images of $Au_xAg_{1-x}@anth$ NPs (a) Ag (9.00 ± 1.62 nm), (b) $AuAg_4$ (10.03 ± 0.86 nm), (c) Au_2Ag_3 (9.47 ± 0.87 nm), (d) Au_3Ag_2 (7.27 ± 0.67 nm), (e) Au_4Ag (9.56 ± 0.56 nm).

Optical Properties of the Hybrid System

$Au_xAg_{1-x}@anth$ NPs were excited at three different wavelengths, which are 350 nm, 367 nm and 390 nm, respectively, according to the three absorption maxima of the anthracene molecule. The fluorescence intensity of the samples at 350 nm excitation follows a descending order for Au_4Ag , $AuAg_4$, Au_2Ag_3 , Ag and Au_3Ag_2 NPs. This trend can be explained by the variance in absorption by the coupled anthracene. It is also possible that anthracene in free ligands also contribute to a portion in absorbing light compared with the coupled fluorophore while emits light less efficiently.

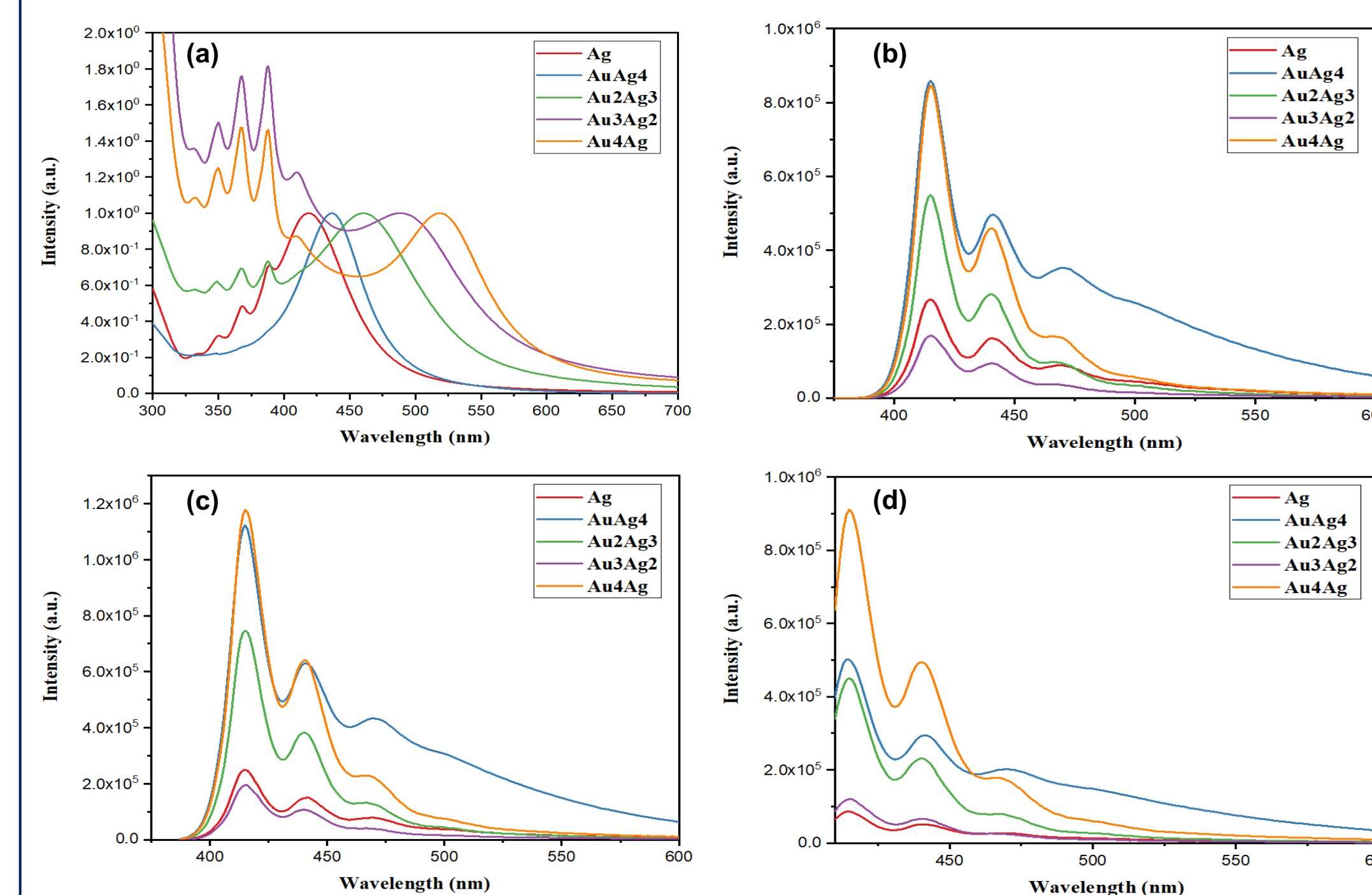


Figure 6. UV-vis and fluorescence spectra of $Au_xAg_{1-x}@anth$ NPs. (a) UV-vis, (b)(c)(d) fluorescence spectra with NPs excited at 350 nm, 367 nm, and 390 nm, respectively.

Conclusion

In summary, relatively homogeneous Au-Ag alloy spherical NPs were synthesized and functionalized with an anthracene-containing ligand. The average size of $Au_xAg_{1-x}@anth$ NPs is 9 nm in diameter. The plasmonic effect on the fluorescence was investigated to be varied among different compositions of the alloy NPs, but also dependent on other factors which includes the dimension of the metal cores and surface coverage of the NPs. More work needs to be done including understanding the difference in light absorption of the samples and determining the exact absorption efficiency and emission efficiency of the NP-coupled anthracene.

- Yang, H.; Wong, E.; Zhao, T.; Lee, J. D.; Xin, H. L.; Chi, M.; Fleury, B.; Tang, H.-Y.; Gaulding, E. A.; Kagan, C. R.; et al. Charge Transport Modulation in PbSe Nanocrystal Solids by Au_xAg_{1-x} Nanoparticle Doping. *ACS Nano* **2018**, *12*, 9091–9100.
- Elbert, K. C.; Lee, J. D.; Wu, Y.; Murray, C. B. Improved Chemical and Colloidal Stability of Gold Nanoparticles through Dendron Capping. *Langmuir* **2018**, *34*, 13333–13338.